Corrosion behavior of 316L stainless steel arc-coated ZrTiAgN multilayer film in media containing chloride

Chun-Yin Lin[1*1], Mu-Jou Ho[1*1], Cheng-Hsun Hsu[1*2]

[1]*Department of Mechanical and Materials Engineering, Tatung University, Taipei City, 10451 Taiwan*
**Corresponding author: rupert475@gmail.com*

Abstract

Stainless steel is known to undergo pitting corrosion when exposed to media solutions containing chloride ions. In this study, ZrTiAgN multilayer coatings were applied to the surface of 316L stainless steel using a cathodic arc deposition (CAD) process and the bias parameters were varied to explore the effect of different bias voltages (-60V, -120V, and -180V) on the coating microstructure and the corrosion behavior of the coated stainless steel. Two media containing chloride ions, NaCl and HCl solutions, were used for the corrosion tests separately. In addition, EPMA, XRD, and SEM were used to analyze the chemical composition, microstructure, and morphology of the coatings.

The experimental findings indicate that as the bias value increases, the silver (Ag) content decreases. The coating consists of a multilayer structure composed of ZrN and TiN phases, with only minimal amounts of amorphous Ag (0.04-0.1 at.%) doped into the film structure. All three different bias coatings exhibited well adhesion (HF1-HF2). In the corrosion test, the polarization test conducted with a NaCl solution revealed that the ZrTiAgN coating enhanced the corrosion resistance of 316L stainless steel. The specimens treated with a bias of -120V displayed the highest polarization resistance value, indicating the best corrosion resistance. Similarly, the ZrTiAgN coating significantly improved the corrosion resistance of 316L stainless steel in the HCl solution immersion test, with the best results observed in the bias -120V specimen. This outcome aligns with the findings from the polarization test.

Keywords: *Stainless steel, ZrTiAgN, Cathodic arc deposition (CAD), Polarization test , Corrosion resistance*

1. Introduction

As we are well-known, stainless steel has become an essential material in our everyday lives. The focus of this study is AISI 316L stainless steel, which falls within the austenitic stainless steel category. In comparison to other stainless steel variants, AISI 316L stands out due to its superior corrosion resistance [1-3]. In fact, it constitutes approximately 70% of stainless steel applications in daily life. Despite its impressive resistance to corrosion, it's worth noting that severe corrosion can occur if the protective Cr_2O_3 passivation layer on the steel's surface is compromised.

Previously, our research team employed cathodic arc vacuum coating technology to conduct PVD surface modification treatments on the different metallic materials. Consequently, the various coatings applied, including TiN, ZrN, CrN, TiAlN, TiZrN, and AlSiN, could exhibit varying levels of corrosion resistance performance. [4-10].

Therefore, AISI 316L stainless steel was selected as the experimental material in this study. Firstly, a practical heat treatment method was used to form a homogeneous microstructure in the steel to be suitable for engineering applications. Subsequently, the cathodic arc deposition method, which is known for its fast deposition rate and strong adhesion, was used. High-quality ZrTiAgN ceramic hard films with excellent corrosion protection were prepared by adding antimicrobial elements such as Ag, Ti, and Zr (especially Ag) [11].

*[1]Doctoral Student, Tatung University
*[2] Professor, Tatung University

2. Experimental

2.1 Material preparation

The material used in this study is AISI 316L stainless steel, which was purchased from Shangsheng Industrial Co., Ltd., and cut into the circular specimens with a diameter of 25mm and height of 6mm.

2.2 Pre-coating heat treatment

Before grinding and polishing, the AISI 316L stainless steel specimens were subjected to practical solution treatment, and the temperature was set to 1050°C in an air furnace for 1 hour. After 1 hour heating, the specimens were quickly removed with the water quenching from the heating furnace.

2.3 Cathodic arc deposition (CAD)

In this study, the ZrTiAgN ceramic hard film was coated on the surface of AISI 316L stainless steel substrates by cathodic arc deposition (CAD) [12,13]. The coating conditions are listed in Table 1.

Table 1 CAD processing parameters for ZrTiAgN coatings in this study.

Parameters	Values
Targets (Wt.%)	Zr(99.99%),TiAg(95%-5%)/Ti(99.99%)
Zr cathode current	90 (A)
TiAg cathode current	60 (A)
Working pressure	$2.5x10^{-2}$ (torr)
Ar+ bombardment	-700/10 (V/min)
Substrate bias	-60, -120, -180 V
Rotation rate	4 (rpm)
Distance between targets and substrates	150 (mm)
Deposition time	50 (min)

Substrate temperature	200~250 (℃)

2.4 Composition, structure and morphology analysis

Quantitative analysis of the film was performed using an electron probe microanalyzer (EPMA). The low-grazing angle thin-film X-ray diffractometer (D8 Discover with GADDS) was used for structural analysis to understand the structure of the film. A field emission scanning electron microscope (FESEM) was used to observe the surface morphology, droplets and holes of the coatings.

2.5 Roughness analysis

A surface roughness meter (Mitutuyo Surf test SV-400) was used to measure the surface roughness of the coated specimens. Five points were measured for each specimens, and calculated the average value.

2.6 Adhesion test

According to the German standard VDI3198[14], this test used a Rockwell hardness machine to conduct an HRC indentation test on the surface of the specimens, and then used SEM to observe the rupture pattern and damage of the indentation of the film, and evaluated its adhesion according to the specification. Then the ASQ (adhesion strength quality) grade was judged by the trace classification.

2.7 Polarization corrosion test

In this study, the EG&G 362 three-electrode method was used for electrochemical polarization experiments. The reference electrode was a Silver-silver chloride electrode, the auxiliary electrode was a platinum (Pt) electrode, and the specimen was a working electrode. Corrosive medium was 3.5wt% NaCl. The starting potential was set from -0.7V to ending potential +0.3V, scanning rate was 0.5mV/s, scanning area was 1cm^2, the Tafel curve obtained from the electrochemical corrosion test was analyzed by software to obtain the corrosion potential (Ecorr), corrosion current (Icorr), and polarization resistance (Rp) [15,16].

3. Results and discussion

3.1 Substrate metallography

Too high solution temperature can directly lead to coarse grains, so 1050°C is the suitable solution temperature for 316L [17]. In this study, AISI 316L was solution treated, held at 1050°C for 1 hour and quenched in water. The metallographic microstructure of 316L stainless steel after solution treatment and without solution treatment was observed by optical microscope (OM), as shown in Fig. 2. Because the 316L stainless steel without solution treatment is a rolled material, it forms a twin crystal structure after solution treatment.

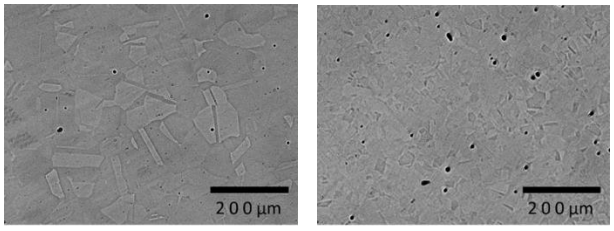

(a) (b)

Fig. 1 Microstructure (50x) of the 316L substrate with and without solid-solution treatment (a) O, and (b) 316L.

3.2 Composition and structure analysis

The results of EPMA analysis are listed in Table 2. As the bias voltage decreases, we can see that the content of silver (Ag) element in the ZrTiAgN film tends to increase gradually.

Table 2 Chemical composition of the coatings analyzed by EPMA (at%).

Specimen	Zr	Ti	N	Ag
-60V	40.56 ±0.574	30.01 ±0.725	29.33 ±0.497	0.10 ±0.006
-120V	38.11 ±0.368	30.61 ±0.279	31.22 ±1.007	0.06 ±0.007
-180V	48.77 ±1.120	26.65 ±0.928	24.54 ±0.783	0.04 ±0.007
ZrTiN	30.64 ±0.731	33.66 ±0.385	35.70 ±0.947	0

The results of XRD analysis to compare the JCPDS cards show that the structure of ZrTiN coated specimen without silver (Ag) element can find the characteristic peaks of Ti_2N (200), ZrN (111), ZrN (200), ZrN (220), and ZrN (311) in the XRD pattern as shown in Fig.2 [18]. On the other hand, The XRD patterns of other Ag-containing coatings are similar to that of Ag-free one. It can be inferred from this result that the trace Ag exists in the coating in an amorphous form.

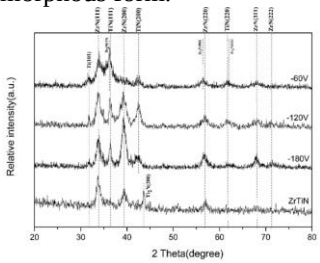

Fig. 2 XRD patterns of various coated specimens.

3.3 SEM surface morphology observation

The observation results for the surface morphology of the specimens are shown in Fig. 3. As can be seen from the micrographs, the uncoated specimen has a smooth surface (Fig.3 a). But after CAD coating, the surface of the specimens produces many micro-droplets, which can affect the surface roughness as shown in Fig.3 (b)-(e). Especially, the coated specimens containing Ag.

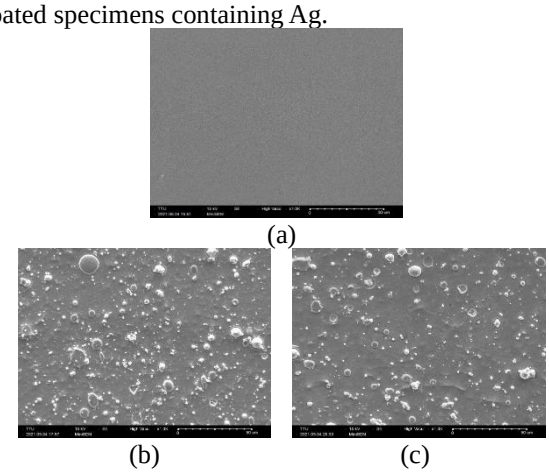

(a)

(b) (c)

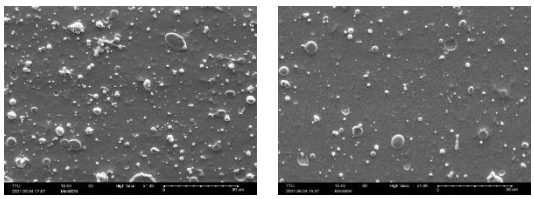

(d) (e)

Fig. 3 SEM surface morphologies (1000x) of the substrate and the coated specimens (a)O, (b) -60V, (c) -120V, (d) -180V, (e) ZrTiN.

3.3 Surface roughness analysis

The surface roughness analysis results are listed in Table 3. The stainless steel substrate has been ground and polished so that the surface roughness is the lowest. There are relatively more droplets at the bias voltage -60V, resulting in the highest surface roughness value.

Table 3 Surface roughness of substrate and the coated specimens.

Specimen	O	-60V	-120V	-180V	ZrTiN
Ra(μm)	0.207 ±0.002	0.508 ±0.058	0.431 ±0.063	0.412 ±0.065	0.3142 ±0.03

3.3 Adhesion analysis

The test was carried out with reference to the German standard VDI 3198, The specimens for this test in the study were designated as HF1 and HF2, as shown in Table 4.

Table 4 Adhesion strength quality (ASQ) for the coatings.

Specimen	-60V	-120V	-180V	ZrTiN
ASQ	HF2	HF1	HF2	HF2

3.4 Polarization test analysis

The polarization curves of the specimens are depicted in Fig. 4. The results reveal that the polarization resistance is notably elevated at bias voltages of -120V and -180V. Remarkably, at -180V bias voltage, the Ecorr value reaches its zenith, while the Icorr value drops to its nadir. This observation underscores that the bias voltage of -180V confers the highest corrosion resistance.

It is evident that the occurrence of pitting corrosion is slightly reduced at bias voltages of -120V and -180V compared to other biases. This finding substantiates that the addition of a small quantity of silver (Ag) atoms effectively enhances corrosion resistance. Additionally, the multilayer film acts as an efficient barrier, preventing corrosive media from penetrating directly into the substrate, consequently bolstering corrosion resistance.

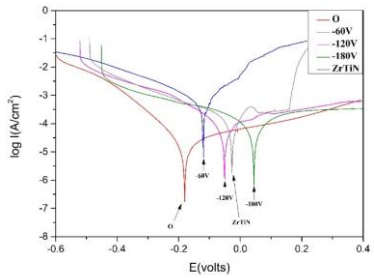

Fig. 4 The polarization curves of substrate and the coated specimens.

4. Conclusions

1. The difference of the bias value affected the Ag content in the film, and the Ag content decreased with the increase of the bias value.
2. Observing the surface morphology of the film by SEM, it can be found that as the Ag content increases, the microdroplets tend to increase, and the roughness is also the largest at the bias voltage -60V with the highest Ag content.
3. Adhesion test showed that all the coated specimens have good adhesion.
4. In the polarization test, the pitting corrosion at the bias voltage of -120V is slightly lighter than that of the others, which proves that the addition of a small amount of Ag atoms can effectively improve the corrosion resistance, and the multilayer film can effectively prevent the corrosion medium from directly penetrating into the substrate, thereby improving corrosion resistance.

Acknowledgments

This research is partially supported by the National Science and Technology Council, Taiwan, R.O.C. under Grant no. MOST110-2221-E-036-006.

References

[1] Y. Wang, Z. Wang, W. Wang, B. Ma: Mater. Sci. Eng. A **884** (2023) 145549.

[2] M. Naeem, S. Awan, M.Shafiq,H.A. Raza, J. Iqbal, J.C. Díaz-Guillén, R.R.M. Sousa, M. Jelani, M. Abrar : Ceram. **48** (2022) 21473-21482.

[3] M. Zeng,Y. Yang, M. Li : Int. J. Electrochem. Sci. **16** (2021) 210723.

[4] C.H. Hsu, H.T. Liu, W.C. Huang, M.R. Lin: Surf. Coat. Technol. **2** (2015) 93-99.

[5] C.H. Hsu, K.H. Huang, M.R. Lin: Surf. Coat. Technol. **259** (2014) 167-171.

[6] C.H. Hsu, K.H. Huang, Y.H. Lin: Wear **306** (2013) 97-102.

[7] W.Y. Ho, C.H. Tsai, C.H. Hsu, W.Y. Ho: Adv Mat Res **415** (2012) 1938-1941.

[8] C.H. Hsu, C.Y. Lee, Z.H. Lin, W.Y. Ho, C.K. Lin: Thin Solid Films **519** (2011) 4928-4932.

[9] C.H. Hsu, K.L. Chen, Z.H. Lin, C.Y. Su, C.K. Lin: Thin Solid Films **518** (2010) 3825-3829.

[10] W.Y. Ho, C.H. Hsu, M.H. Tsai, Y.S. Yang, D.Y. Wang: Appl. Surf. Sci. **256** (2010) 2705-2710.

[11] H. Xiang, D. Liu, X. Chen, H.Cao, X. Dong, Mater.Express **9**(9) (2019) 1067-1075.

[12] A. Bjerke, F. Lenrick, A. Hrechuk, K.S, R.M. M. Andersson, V. Bushlya: Wear **532-533** (2023) 205093.

[13] Naddaf, B. Abdallah, M. Ahmad, M. A-Kharroub: Nucl Instrum Methods Phys. Res. B **381(**2016) 90-95.

[14] B. Lenz, H. Hasselbruch, A. Mehner: Surf. Coat. Tech. **385** (2020) 21-23.

[15] Q. Xiao, J. Chen, H.B. Lee, C.H. Jang, K. Jang: Corros. Sci. **210** (2023)110830.

[16] D. Jaiswal, D. Pathote, V. Singh, C.K. Behera: Mater. Today, **1** (2023) 221005.

[17] K.N. Tsai, S.Y. Hsu, Y.T. Lai, S.Y. Chang, S.Y. Tsai, J.G. Duh: Surf. Coat. Tech. 453 (2023) 129123.

[18] J. Senthilselvan, R. R. Pillai, R.K. , B. Baskar , K. Valleti, J. Manonmani : Ceram. Int. ,(2023)